TR-87-10

The Kinematics of Robotic Bevel-Gear Trains

by

Lung-Wen Tsai

THE KINEMATICS OF ROBOTIC BEVEL-GEAR TRAINS

Lung-Wen Tsai
Associate Professor

Mechanical Engineering Department/
Systems Research Center
The University of Maryland
College Park, Maryland 20742

Member of the ASME

Abstract

A systematic approach has been developed for the kinematic analysis of multi-degree-of-freedom robotic bevel-gear trains. The approach is based on the idea that the motion of the end-effector can be described by an equivalent open-loop chain and that the relative rotations between every two adjacent links in the equivalent open-loop chain can be derived from a set of fundamental circuit equations. The theory is demonstrated by the kinematic analysis of a robotic wrist.

Introduction

In order to position and orient the end-effector of a manipulator arbitrarily in space, it is necessary that a manipulator has six degrees of freedom. If we limit ourself to single degree-of-freedom joints, then an open-loop manipulator must have six joints and seven links. The first three joints, starting from the base, are commonly designed to perform gross motion of the end-effector, and the remaining joints are used to perform fine manipulation. For this reason, the first three moving links are commonly called the arm, while the last three moving links the wrist. The kinematic analysis of an open-loop robot manipulator has been studied thoroughly in recent years. See, for examples, references 5, 12 and 17.

Although open-loop manipulators are popular in itself, in practice many manipulators are constructed in a partially closed-loop configuration to ease the actuator design and/or to reduce the inertia loads on the actuators. For example, the Cincinnati Milacron T^3 uses a three roll wrist mechanism which is made of a closed-loop bevel-gear train [15], while Bendix Corporation used a Roll-Bend-Roll type bevel-gear wrist mechanism [2]. In contrast to the open-loop design, a manipulator with partially closed-loop configuration has more than six joints and the joints may be revolute, prismatic and/or gear pairs. The kinematic and dynamic analysis is, therefore, more complicated than that of an open-loop type.

Various methods for deriving the displacement equations for spur-gear trains can be found in the literature [1,3,4,6-9,11,13,14,16]. Perhaps, the most promising approach is the systematic method first introduced by Freudenstein [6]. The method utilizes the concept of fundamental circuits. The method was elaborated in more detail by Freudenstein and Yang [8]. And recently, a computer algorithm was developed by Tsai [16].

In bevel-gear trains, the analysis is more complex due to the three dimensional motion of the gears and arms. Day, et al. [4] carried out the analysis of a bevel-gear train using the concept of fundamental circuit. However, the motion of the arm is limited to a rotation about a fixed axis. Freudenstein, et al suggested a tabular method and a general procedure for applying the method was outlined [7]. In this paper, it is shown that the fundamental circuit equations can be applied to the analysis of bevel-gear trains using the concept of relative rotation. The principle is illustrated by an example.

Kinematic Structure

Functional Representation

This is essentially the schematic drawing of the mechanism. Shafts, bearings, gears and other elements are drawn similar to their mechanical construction. For reasons of clarity and simplicity, only functional elements essential to the structure are shown.

Fig. 1a shows the functional representation of a robotic bevel-gear train resembling the Cincinnati Milacron T^3 wrist mechanism [15]. The mechanism has three coaxial inputs, i.e. links 2, 6 and 7. Bevel gears 4, 5, 6 and 7 transmit these rotations to the end-effector attached to link 4 and housed in the carrier 3. The axis locations of the turning pairs are as follows:

Axis a : pairs 1-2, 2-7, and 7-6
Axis b : pairs 2-5 and 3-5
Axis c : pair 3-4

Together, this mechanism contains 7 links, 6 turning pairs and 3 gear pairs. The three axes a, b and c intersect at a point O as shown in Fig. 1a. The end-effector possesses a spherical motion with three degrees of freedom.

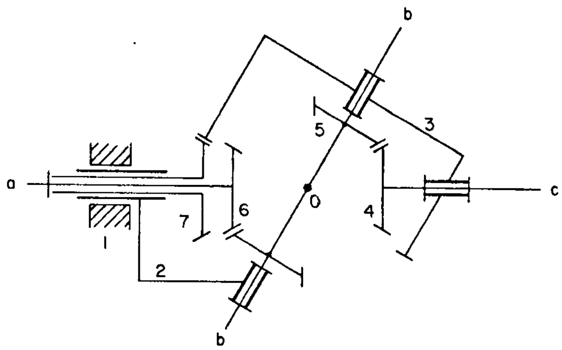

Fig. 1a. Functional schematic of a robotic bevel-gear train.

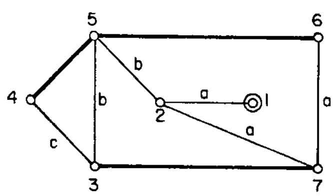

Fig. 1b. Graph representation of Fig. 1a.

Graph Representation

In the graph representation, links are denoted by vertices and joints by edges. In order to distinguish a turning-pair connection from a gear-pair connection, turning pairs are represented by thin edges and gear pairs by heavy edges. The thin edges are labeled according to their axis locations. Fig. 1b shows the graph representation of the gear train shown in Fig. 1a.

From the graph of Fig. 1b, we observe that there are three f-circuits (fundamental circuits): (4,5)(3); (5,6)(2); and (3,7)(2). In this notation, the first two numbers for each circuit designate the gear pairs and the third identifies the arm. See References 3 and 6 for the definition of fundamental circuit and how to identify the arm, which is called the transfer vertex.

Canonical Representation

When there are three coaxial links in a mechanism such as links 2, 3 and 5 shown in Fig. 1a, it is always possible to reconfigure the turning-pairs among the three links without affecting the functionality of the mechanism. Fig. 2a shows the turning-pair connections among links 2, 3 and 5 in its original form. Figs. 2b and 2c show two alternative connections. The number of alternative connections increases with the number of coaxial links. This suggests a canonical representation for the graph and its corresponding functional schematic.

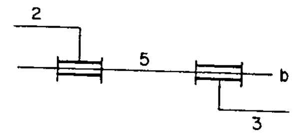

Fig. 2a. Three coaxial links

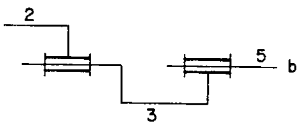

Fig. 2b. First alternative

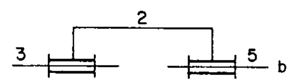

Fig. 2c. Second alternative

Recall that a "walk" of a graph is an alternating sequence of vertices and edges beginning and ending with vertices, and a "path" is a walk in which all the vertices are distinct. Also recall that the subgraph obtained by deleting all the geared edges from an epicyclic-gear train is a tree. A path made of only thin edges is called a thin-edged path. In this paper, we shall choose the graph representation in which all the thin-edged paths originating from the ground link have distinct edge labels as the canonical graph, and the corresponding functional representation as the canonical schematic. The graph shown in Fig. 1b is not canonical since the 2-5 and 5-3 edges in the path 1 → 2 → 5 → 3 → 4 are of the same label. On the other hand, the graph shown in Fig. 3b is canonical. There are six thin-edged paths originating from vertex 1, namely, 1 → 2, 1 → 2 → 3, 1 → 2 → 3 → 4, 1 → 2 → 5, 1 → 6 and 1 → 7. Each of these six paths have distinct edge labels. The corresponding canonical representation of the mechanism schematic is shown in Fig. 3a.

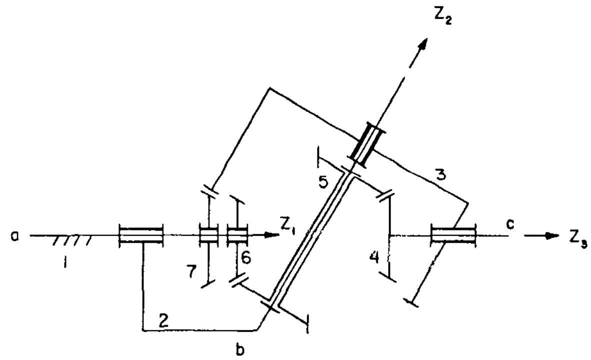

Fig. 3a. Canonical schematic of Fig. 1a.

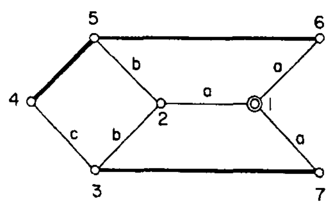

Fig. 3b. Canonical graph of Fig. 3a.

The Equivalent Open-Loop Chain

The tree obtained by deleting all the geared edges from a canonical graph represents an open-loop kinematic chain consisting of links and lower pairs only. The kinematic analysis of any link in an epicyclic gear train can, therefore, be derived by performing the matrix transformation to the open-loop chain starting from the ground link and ending at the link of interest. In particular, we define the thin-edged path which starts from the ground link and ends at the end-effector link as the "equivalent open-loop chain" for the wrist. Fig. 4 shows the equivalent open-loop chain for the wrist shown in Fig. 1a.

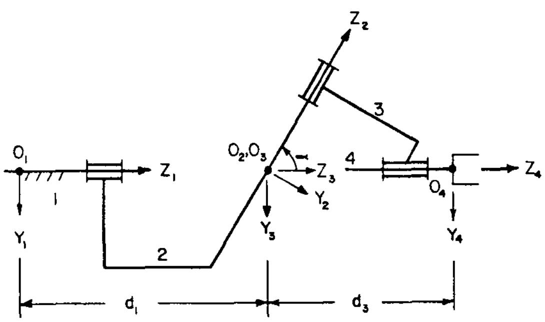

Fig. 4. The equivalent open-loop chain for the wrist mechanism shown in Fig. 1a.

In order to facilitate the analysis, a coordinate system (X_i, Y_i, Z_i) is attached to each link of the equivalent open-loop chain in accordance with the Hartenberg and Denavit convention [10] as shown in Fig. 4. Thus, coordinate system (X_1, Y_1, Z_1) is attached to link 1 (the reference frame); (X_2, Y_2, Z_2) to link 2; (X_3, Y_3, Z_3) to link 3; and (X_4, Y_4, Z_4) to link 4 (the end-effector). The origin of the first coordinate system is to be chosen at the intersection of the Z_1-axis and the common normal between Z_1-axis and the last axis of the arm. In Fig. 4, the origin O_1 and the X_1-axis have been chosen arbitrarily since we do not know how the wrist is attached to the hand at this time. Also, the X_i, i=1 to 4, axes are not shown in Fig. 4, since they are all perpendicular to both Y_i and Z_i axes according to the right-hand-screw rule. The Hartenberg and Denavit parameters for the equivalent open-loop chain of the Cincinnati Milacron T^3 wrist are given in Table I.

Table I. Hartenberg and Denavit Parameters for the Cincinnati Milacron T^3 Wrist Mechanism

i	a_i	α_i	d_i
1	0	α	d_1
2	0	$-\alpha$	0
3	0	0	d_3

where a_i and α_i denote the offset distance and the twist angle between axes Z_i and Z_{i+1}, respectively, and d_i denotes the translational distance along the Z_i axis.

The equivalent open-loop chain shown in Fig. 4 has been sketched in the configuration in which all the X_i, i = 1 to 4, axes are parallel to each other and pointing out of the paper. We shall denote this position as the "zero position" of the wrist mechanism, and refer to the displacement of a link (or a gear) in the mechanism as the rotation of the link with respect to this reference position, positive or negative in accordance with the right-hand-screw rule.

We note that in order to analyze the equivalent open-loop chain, we need to know the relative angular displacements of links 4 to 3, 3 to 2, and 2 to 1. These relative angular displacements are to be derived from the fundamental circuit equations described in the next section.

Fundamental Circuit Equations

Let i, j denote the vertices of a gear pair in an f-circuit in which k is the transfer vertex. Then links i, j and k constitute a simple epicyclic gear train, and the following fundamental circuit equation applies:

$$\theta_{ik} = N_{ji}\,\theta_{jk} \tag{1}$$

where θ_{ik}, θ_{jk} denote the relative angular displacements of gears i and j with respect to the arm k, and N_{ji} denote the gear ratio of the gear pair ij. $N_{ji} = + T_j/T_i$, if a positive rotation of gear j with respect to the arm k produces a positive rotation of gear i; and $N_{ji} = -T_j/T_i$, otherwise, where T_j and T_i denote the number of teeth on gears j and i respectively, and the sense of rotation is defined by applying the right-hand-screw rule to the rotation of a gear about its Z axis. By definition, $\theta_{ij} = -\theta_{ji}$ and $N_{ij} = 1/N_{ji}$ for all i and j. Equation (1) is valid whether the gear train is of spur-gear type or bevel-gear type, and whether the arm is fixed or rotating. We can write Eq. (1) once for each f-circuit in the mechanism. For the gear train shown in Fig. 1 we have

F-circuit (4,5)(3), $\theta_{43} = N_{54}\,\theta_{53}$ (2)

F-circuit (5,6)(2), $\theta_{52} = N_{65}\,\theta_{62}$ (3)

F-circuit (3,7)(2), $\theta_{32} = N_{73}\,\theta_{72}$ (4)

where $N_{54} = -T_5/T_4$, $N_{65} = -T_6/T_5$, and $N_{73} = T_7/T_3$.

We observed that θ_{43} and θ_{32} in Eqs. (2) - (4) are the relative angular displacements needed for the analysis of the equivalent open-loop chain, and, θ_{53}, θ_{62}, θ_{72} and θ_{52} are unknown angular displacements which should be expressed in terms of the three inputs: θ_{21}, θ_{61} and θ_{71}. This can be accomplished by the following coaxial conditions.

Coaxial Conditions

Let i, j and k be three coaxial links, then the relative angular displacements among these three links are related by the following condition:

$$\theta_{ij} = \theta_{ik} - \theta_{jk} \quad (5)$$

where θ_{ij} denote the relative angular displacement of link i with respect to link j. For the mechanism considered, we have

$$\theta_{53} = \theta_{52} - \theta_{32} \quad (6)$$

$$\theta_{62} = \theta_{61} - \theta_{21} \quad (7)$$

and

$$\theta_{72} = \theta_{71} - \theta_{21} \quad (8)$$

The Displacement Equations

The fundamental circuit equations along with the coaxial conditions completely define the relative angular displacements of the bevel-gear train. The equations are linear which can be solved in closed form or by computer algorithms. For the mechanism shown in Fig. 1a, the analysis is given as follows.

Substituting Eq. (8) into (4), yields

$$\theta_{32} = N_{73}\,(\theta_{71} - \theta_{21}) \quad (9)$$

Substituting Eq. (7) into (3), yields

$$\theta_{52} = N_{65}\,(\theta_{61} - \theta_{21}) \quad (10)$$

Substituting Eqs. (9) and (10) into (6) and then the resulting equation into (2), yields

$$\theta_{43} = N_{54}\,[N_{65}\,(\theta_{61}-\theta_{21}) - N_{73}\,(\theta_{71}-\theta_{21})] \quad (11)$$

Equations (9) and (11) express the rotation of the end-effector about the Z_2 and Z_3 axes in terms of the three input displacements: θ_{21}, θ_{61} and θ_{71}. The position and orientation of the end-effector with respect to the frame, the (X_1, Y_1, Z_1) coordinate system, can be obtained from the following matrix of transformation:

$$T = A_1\,A_2\,A_3 \quad (12)$$

where

$$A_1 = \begin{bmatrix} c\theta_{21} & -c\alpha s\theta_{21} & s\alpha s\theta_{21} & 0 \\ s\theta_{21} & c\alpha c\theta_{21} & -s\alpha c\theta_{21} & 0 \\ 0 & s\alpha & c\alpha & d_1 \\ 0 & 0 & 0 & 0 \end{bmatrix} \quad (13)$$

$$A_2 = \begin{bmatrix} c\theta_{32} & -c\alpha s\theta_{32} & -s\alpha s\theta_{32} & 0 \\ s\theta_{32} & c\alpha c\theta_{32} & s\alpha c\theta_{32} & 0 \\ 0 & -s\alpha & c\alpha & 0 \\ 0 & 0 & 0 & 1 \end{bmatrix} \quad (14)$$

$$A_3 = \begin{bmatrix} c\theta_{43} & -s\theta_{43} & 0 & 0 \\ s\theta_{43} & c\theta_{43} & 0 & 0 \\ 0 & 0 & 1 & d_3 \\ 0 & 0 & 0 & 1 \end{bmatrix} \quad (15)$$

where $c\theta_{ij} = \cos\theta_{ij}$, $s\theta_{ij} = \sin\theta_{ij}$, $c\alpha = \cos\alpha$ and $s\alpha = \sin\alpha$.

Let $\bar{p}_i$ be the position vector of a point in the end-effector and expressed in the ith coordinate system, and let $\bar{u}_i$ be a unit vector that is attached to the end-effector and expressed in the ith coordinate system, then

$$\bar{p}_1 = T\,\bar{p}_4 \qquad (16)$$

$$\bar{u}_1 = T\,\bar{u}_4 \qquad (17)$$

where

$$\bar{p}_i = [p_{xi},\ p_{yi},\ p_{zi},\ 1]^t \qquad (18)$$

$$\bar{u}_i = [u_{xi},\ u_{yi},\ u_{zi},\ 0]^t \qquad (19)$$

and t denotes the transpose of the matrix.

Orientation of the Third Joint Axis:

In the analysis of a robotic wrist, very often we are interested in knowing the orientation of the end-effector. Let $\bar{z}_{31}$ be a unit vector attached to the Z_3-axis and expressed in the 1st coordinate system as shown in Fig. 4, then

$$\bar{z}_{31} = A_1\,A_2\,[0\ 0\ 1\ 0]^t \qquad (20)$$

Substituting Eqs. (13) and (14) into (20), yields

$$\bar{z}_{31} = \begin{bmatrix} -S\alpha C\theta_{21}S\theta_{32} - S\alpha C\alpha S\theta_{21}C\theta_{32} + S\alpha C\alpha S\theta_{21} \\ -S\alpha S\theta_{21}S\theta_{32} + S\alpha C\alpha C\theta_{21}C\theta_{32} - S\alpha C\alpha C\theta_{21} \\ S^2\alpha C\theta_{32} + C^2\alpha \\ 0 \end{bmatrix} \qquad (21)$$

Orientation of the Second Joint Axis:

Similarly, let $\bar{z}_{21}$ be a unit vector attached to the Z_2-axis and expressed in the 1st coordinate system, then

$$\bar{z}_{21} = [\ S\alpha S\theta_{21}\quad -S\alpha C\theta_{21}\quad C\alpha\quad 0\ ]^t \qquad (22)$$

We observe that the Z_2-axis can be kept stationary by holding θ_{21} constant. The Z_3-axis can also be kept stationary by holding the rotations of links 2 and 7. Under this condition the end-effector spins about the Z_3-axis via the rotation of gear 6.

The Angular Velocity Equations

The magnitudes of the relative angular velocities between links 3 and 2, and 4 and 3 can be obtained by taking the time derivatives of Eqs. (9) and (11) as shown below:

$$\omega_{32} = N_{73}\,(\omega_{71} - \omega_{21}) \qquad (23)$$

$$\omega_{43} = N_{54}\,[N_{65}\,(\omega_{61} - \omega_{21}) - N_{73}\,(\omega_{71} - \omega_{21})] \qquad (24)$$

where ω_{ij} denote the magnitude of the angular velocity of link i relative to link j, the direction of which is defined along the common Z-axis between links i and j. The angular velocity vector $\bar{\omega}_{41}$, of the end-effector is given as:

$$\bar{\omega}_{41} = \omega_{43}\,\bar{z}_{31} + \omega_{32}\,\bar{z}_{21} + \omega_{21}\,\bar{z}_{11} \qquad (25)$$

where $\bar{z}_{31}$ and $\bar{z}_{21}$ are given by Eqs. (21) and (22), and $\bar{z}_{11}$ is the unit vector along Z_1-axis.

Summary

We have shown that the kinematics of spatial robotic bevel-gear trains can be analyzed in a systematic manner. The procedure is very general and can be applied to the kinematic analysis of any multi-degree-of-freedom bevel-gear train. The procedure can be summarized as follows:

(a) Sketch the functional representation/schematic of the gear train. Number each link and label the axes of the turning pairs.
(b) Determine the degrees of freedom, the input links, and the ground link for the gear train.
(c) Draw the graph of the gear train from which determine the fundamental circuits and the transfer vertices.
(d) Transform both the graph and functional representations into canonical forms and then determine the equivalent open-loop chain for the gear train.
(e) Assign a coordinate system to each link of the equivalent open-loop chain according to Hartenberg and Denavit convention, and then define the zero-position and gear ratios for the gear train.
(f) Derive the relative angular displacement equations for all the fundamental circuits.
(g) Derive the appropriate coaxial conditions.
(h) Solve the angular displacement equations.
(i) Solve the matrix of transformation for the equivalent open-loop chain and obtain the angular velocity equations when necessary.

Acknowledgement

The author is grateful to the Systems Research Center of the University of Maryland for the support of this research through an NSF grant No. NSF-CDR-8500108.

References

1. R.R., Allen, "Multiport Models for the Kinematic and Dynamic Analysis of Gear Power Transmissions," ASME J. of Mechanical Design, Vol. 101, No. 2, pp. 258-267, Apr. 1979.
2. Anonymous, "Bevel Gears Make Robot's "Wrist" More Flexible," Machine Design, Vol. 54, No. 18, p. 55, Aug. 12, 1982.
3. F. Buchsbaum, and F. Freudenstein, "Synthesis of Kinematic Structure of Geared Kinematic Chains and Other Mechanisms," J. of Mechanisms and Machine Theory, Vol. 5, pp. 357-392, 1970.

4. C.P. Day, H.A. Akeel, and L.J. Gutkowski, "Kinematic Design and Analysis of Coupled Planetary Bevel-Gear Trains," ASME J. of Mechanisms, Transmissions, and Automation in Design, Vol. 105, No. 3, pp. 441-445, Sept. 1983.
5. J. Duffy, Analysis of Mechanisms and Robot Manipulators, Wiley, New York, 1980.
6. F. Freudenstein, "An Application of Boolean Algebra to the Motion of Epicyclic Drives," ASME J. of Engineering for Industry, Vol. 93, Series B, pp. 176-182, Feb. 1971.
7. F. Freudenstein, R. W. Longman, and C.-K. Chen, "Kinematic Analysis of Robotic Bevel-Gear Trains," ASME J. of Mechanisms, Transmissions, and Automation in Design, Vol. 106, No. 3, pp. 371-375, Sept. 1984.
8. F. Freudenstein, and A.T. Yang, "Kinematics and Statics of a Coupled Epicyclic Spur-Gear Train," J. of Mechanisms and Machine Theory, Vol. 7, pp. 263-275, 1972.
9. D. Gibson, and S. Kramer, "Symbolic Notation and Kinematic Equations of Motion of the Twenty-Two Basic Spur Planetary Gear Trains," ASME J. of Mechanisms, Transmissions, and Automation in Design, Vol. 106, No. 3, pp. 333-340, Sept. 1984.
10. R.S. Hartenberg, and J. Denavit, Kinematic Synthesis of Linkages, McGraw-Hill, New York, 1964.
11. H.E. Merritt, Gear Trains, Pitman and Sons, London, 1947.
12. D.L. Pieper, and B. Roth, "The Kinematics of Manipulators Under Computer Control," Proceedings II - International Congress on the Theory of Machines and Mechanisms, Vol. 2, pp. 159-168, 1969.
13. J.E. Shigley, and J.J. Uicker Jr., Theory of Machines and Mechanisms, McGraw-Hill, New York, 1980.
14. D. Smith, "Analysis of Epicyclic Gear Trains via the Vector Loop Approach," Proceedings of the Sixth Applied Mechanisms Conference, Denver, Colorado, Paper No. 10, 1979.
15. T. Stackhouse, "A New Concept in Wrist Flexibility," Proceeding of the 9th International Symposium on Industrial Robots, Washington, D.C., pp. 589-599, 1979.
16. L.W. Tsai, "An Algorithm for the Kinematic Analysis of Epicyclic Gear Trains," Proceeding of the 9th Applied Mechanisms Conference, Kansas City, Missouri, Oct. 1985.
17. L.W. Tsai, and A.P. Morgan, "Solving the Kinematics of the Most General Six- and Five-Degree-of-Freedom Manipulators by Continuation Methods," ASME J. of Mechanisms, Transmissions, and Automation in Design, Vol. 107, No. 2, pp. 189-200, June 1985.